Use of Pulsations to Enhance the Distribution of Liquid Injected into Fluidized Particles with Commercial-Scale Nozzles

Aidan Leach, Rana Sabouni, Franco Berruti, and Cedric Briens
Dept. of Chemical and Biochemical Engineering, Institute for Chemicals and Fuels from Alternative Resources (ICFAR), The University of Western Ontario, London, ON, Canada N6A 5B9

DOI 10.1002/aic.13872
Published online July 6, 2012 in Wiley Online Library (wileyonlinelibrary.com).

Gas-atomized liquid injections into fluidized beds are commonly used in industrial processes such as fluid coking, fluid catalytic cracking (FCC), and pharmaceutical granulation, where it is important to optimize the distribution of the injected liquid to prevent the formation of unwanted liquid–solid agglomerates and maximize product yields. This injection is typically a two-phase, gas-atomized liquid injection. One issue with such a liquid injection is that most of the liquid is deposited at the end of the jet tip within the reactor. This study proposes introducing artificial fluctuations into the injection flow, which causes the jet penetration to vary, allowing for a more even spread of liquid throughout a fluidized bed reactor. The effect of artificial pulsations in the atomized injection, of various frequency and amplitude, was investigated in this study. Using pulsations, greatly enhanced the liquid distribution on the bed particles. © 2012 American Institute of Chemical Engineers *AIChE J,* 59: 719–728, 2013
Keywords: fluidization, spray nozzles, pulsations

Introduction

Gas-atomized liquid feeds are used in many industrial gas–solid fluidized bed reactors. These injections are used to either introduce feedstocks or coolants into a wide variety of chemical reactors. Some examples include fluid cokers, fluid catalytic crackers (FCC), and gas-phase polymerization reactors. In the fluid coker units, such as the ones used to produce synthetic crude from the Athabasca oil sands of Northern Alberta, heavy bitumen is mixed with steam, and then injected into a fluidized bed of coke particles. The steam helps break the bitumen into droplets, and then helps disperse it into the bed. This reaction takes place at $\sim$530°C.[1] Bitumen is heated on contact with the coke and, after achieving sufficiently high temperatures, its large hydrocarbon molecules are thermally cracked into smaller, more valuable products. The efficiency and product yields of this reactor system are highly dependent on the effectiveness of the liquid-solid contact that occurs immediately after the liquid injection.[2]

Although maximizing solid-liquid contact is critical in processes where most of the liquid vaporizes immediately after the injection,[3] such as FCC or polymerization reactors, it is even more important in processes where the injected liquid does not evaporate quickly, and the main reactions occur in the liquid-phase, such as fluid coking. In addition, fluid coking is endothermic and it is, therefore, of great importance to maximize the performance of the injection nozzle, to spread the liquid as efficiently as possible and minimize mass and heat-transfer limitations, to allow the reactions to proceed quickly and efficiently.[4] In fluid coking, it has been seen that a more uniform distribution of liquid, on the largest possible number of particles, results in higher yields of valuable products, making the unit more efficient and profitable.[5] Previous studies have shown that the ideal liquid distribution is achieved when the liquid forms a thin uniform film over the solid particles.[2] This ideal case is not feasible in large industrial units, where the injected liquid does not evenly coat the solid particles.[5] What happens in reality is that liquid–solid agglomerates form on the injection, trapping the liquid feed. This trapped liquid reacts slowly, hindering the kinetics of the cracking reactions. Although many of the agglomerates break apart quickly as a result of rigorous mixing in the fluidized bed, hastening the reaction, stronger agglomerates will persist, continue to limit the reaction, and could negatively affect the quality of fluidization.[6] These agglomerates were detected using x-ray analysis.[7] In a more recent study,[2] a sucrose solution was used in the injection, to recover the agglomerates and determine their strength and other properties.

One potential factor which could influence the quality of the performance of injection nozzles is the presence of fluctuations in the injection flow rate. Several studies have investigated the effects of nozzle pulsations on the quality of liquid–solid contact efficiency. A previous study[8] used local triboelectric probes placed throughout a liquid jet to determine the consistency of the liquid spray over the course of an injection. These small probes measured the electrical

Correspondence concerning this article should be addressed to C. Briens at cbriens@uwo.ca.

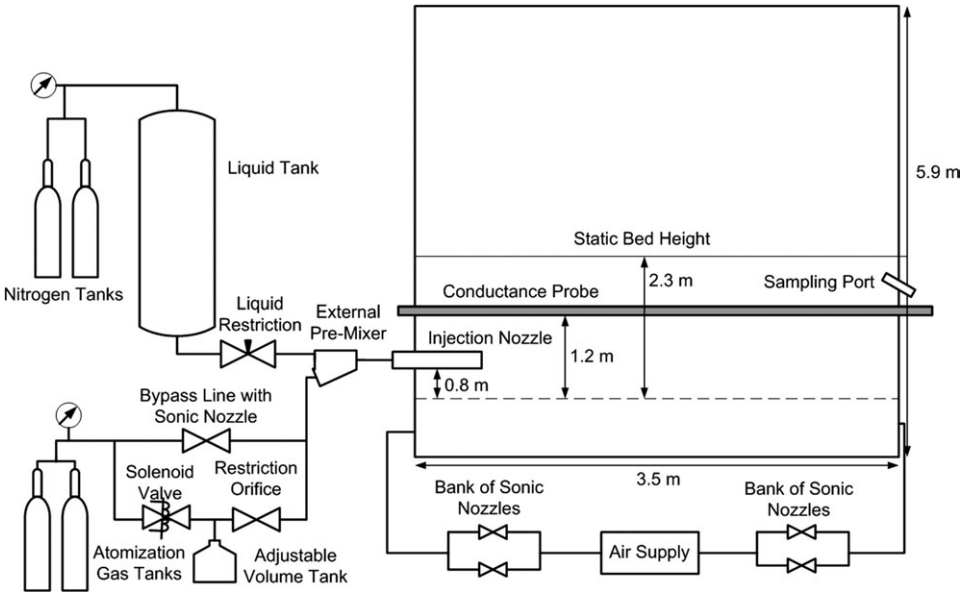

Figure 1. Schematic diagram of experimental apparatus.

signal produced by the physical contact between moving particles (through the triboelectric effect). The presence of liquid changed the amount of electricity produced. The study found that pulsations in the gas-liquid spray jet are caused by unstable flow through the nozzle, and these pulsations tend to reduce the quality of the liquid-solid contact. A further study[9] found that these pulsations occur in the same fashion in open-air tests as they do in a fluidized bed. As such, the pulsations are not caused by the turbulence or chaotic flow within the fluidized bed, but, rather, primarily by the conditions upstream of the spray nozzle tip. Also, this allowed for calibrations of future pulsation systems, such as the ones presented in this study, to be performed in open air.

Another study[10] assumed that stable, nonpulsating sprays are required for optimal reactor operation. A limitation of this study is that it only attempted very severe pulsations, when the spray alternated between well-atomized liquid droplets, and a liquid-only injection. McDougall et al.[11] then used several techniques to measure the quality of fluidization in a fluidized bed, such as measuring the bubble size at the transport disengaging height in the bed, dropping a ball through the fluid bed and measuring the settling velocity, and determining the liquid–solid agglomerates content in the bed by measuring the fines leaving the bed. It was found that pulsating sprays reduced the bed fluidization quality and promoted agglomerate formation. That study did not directly measure liquid–solid contact.

Sabouni et al.[12] used the active conductance technique from a previous study[13,14] to study the effect of nozzle pulsations on the quality of liquid-solid contact in a laboratory scale fluidized bed. The study focussed on gas-line pulsations that were milder than those of previous studies and where the instantaneous gas-to-liquid (G/L) ratio in the nozzle was never reduced all the way to 0 wt %. These pulsations led to a dramatic increase in nozzle performance. The purpose of this study is to build on this study, and to test it with commercial scale nozzles in a large-scale fluidized bed, under a wide variety of operating conditions.

Experimental Apparatus

Experiments were performed in a wedge-shaped fluidized bed. The bed had two parallel sides with lengths of 0.2 and 1.2 m, spaced 3.5 m apart (Figures 1 and 2). The walls of the bed were made of steel and were electrically grounded. Air was used as a fluidizing gas, and its flow rate was controlled with a system of four parallel sonic nozzles. The relative humidity of the fluidization air was held constant at $\sim$12% and entered the system at a constant temperature of 20°C.

The fluidized bed was filled with silica sand particles with a Sauter mean diameter of 190 μm and a particle density of 2600 kg/m^3. These particles are Group B particles according to Geldart's powder classification system. They are not porous particles. These are both characteristics shared with coke particles, and silica sand is perfectly wettable with water, as coke is perfectly wettable with oil, making silica sand a good choice for an industrial comparison. The bed had a static height of 2.3 m and contained 8800 kg of sand.

Probes and data acquisition

Type J thermocouples were used in the bed to monitor the temperature of the air entering and leaving the system, as well as the temperature of the bed itself. To ensure accurate data, 18 thermocouples were used in total, in various locations in the bed. The thermocouples had a penetration depth of 2.5 cm.

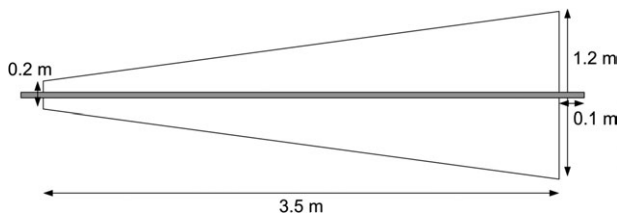

Figure 2. Dimensions of experimental apparatus (top view) with placement of conductance probe in gray.

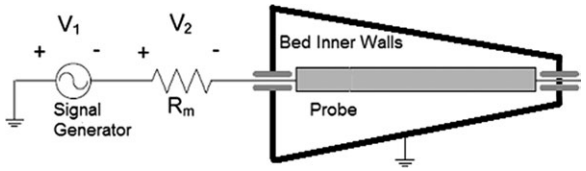

Figure 3. Placement and corresponding circuit for the conductance probe.

The electrode used as the conductance probe was a stainless steel tube with an outer diameter of 7 mm and a thickness of 1 mm. It was placed 1.2 m above the distributor grid in the fluidized bed and ran through the long side of the bed, hanging out 10 cm on each side (as shown in Figures 1 and 2). A similar probe was used in previous studies,[13,14] but in this study a probe was used that was large enough to run throughout the entire unit. This was necessary due to the high forces present in a larger fluidized bed. The tube was held in place with nylon fittings so that it was electrically insulated from the grounded bed walls (Figure 2). The probe was connected to a 51-kΩ resistor. Figure 3 shows a schematic diagram of the conductance probe.

Active conductance technique

A function generator was used to apply a sinusoidal electrical signal to the conductance probe. Its sinusoidal signal had an root mean square (RMS) voltage of 6.7 V. With reference to Figure 3, the conductance of the bed could be determined by using the ratio of the voltage across the resistor (V_2) and the voltage produced by the function generator (V_1), by using Ohm's law:

$$R_{\text{bed}} = 1/\Gamma_{\text{bed}} = R_{\text{m}} \times (V_1/V_2 - 1) \tag{1}$$

where R_{bed} is the electrical resistance of the bed and Γ_{bed} is its electrical conductance, and R_{m} is the known resistance of the resistor in the system (51 kΩ).

A data acquisition system recorded the voltages V_1 and V_2, the thermocouple readings, and the signals from the pressure transducers measuring the gas and liquid pressures in the injection and the differential pressure across the bed, from which the bed height could be estimated. The data was sampled at 1000 Hz during the injection and defluidization, but the sampling frequency was reduced to 100 Hz during drying.

The liquid was injected through a commercial-scale nozzle illustrated in Figure 4, which was placed 1 m above the gas distributor, in the centre of the smaller (0.2 m) wall of the bed (see Figure 1). This nozzle has been patented for fluid coking applications,[15] and was used in previous studies by the authors.[14,16]

Deionized water was used as the liquid for the injections, due to its high purity. This purity was required to prevent an accumulation of impurities over the course of several experiments. The liquid flow rate was controlled by regulating the nitrogen pressure applied to the liquid feed tank. The time-averaged liquid flow rate was 2.2 kg/s for all the experiments of this study. A gas mixture of 18% nitrogen and 82% helium by mass was used for the atomizing gas. This was chosen because the combination of these mixed gas, deionized water, and silica sand provides a realistic approximation of the steam, bitumen, and coke system used in industrial fluid coking units. The gas flow rate was controlled using a restriction orifice. Pressure transducers were used to measure the pressure on both sides of the orifice, and, using calibration data, the instantaneous flow rate could be determined from the instantaneous pressures.

The gas and liquid were mixed in an external premixer upstream of the spray nozzle. Two types of premixer were used: a bilateral flow conditioner (BFC) and a W premixer. In the BFC, the water and gas enter from different sides, both at an angle of 30° with respect to the axis of the nozzle. The pressure in the premixer was monitored with a pressure transducer.

Solenoid valve

To induce pulsations in the liquid spray, a solenoid valve was introduced in the atomizing gas line, just upstream of the restriction orifice (Figure 1). The volume between the solenoid valve and the restriction orifice was varied in the experiments to change the pulsations amplitude. This solenoid valve was controlled by a function generator using the circuit shown in Figure 5. The function generator produced a square-wave electrical voltage. Because of the nature of the transistor in the circuit, the solenoid valve is opened when the signal is at its high setting and closed when the signal is low. The high and low periods have an equal period, which can be controlled by changing the frequency of the square wave signal. By opening and closing the gas line, the (G/L) ratio is no longer held constant, and the fluctuations in gas pressure in the line cause the water flow rate to also change. This induces the pulsations whose effects were investigated in this study. The pulsation frequency was fast enough that the gas flow rate never decreased to zero, as there was still a release of gas from the region between the solenoid valve and the restriction orifice governing the gas flow rate. In addition, the gas flowing through the bypass line (Figure 1) ensured that there was always a significant gas flow to the spray nozzle.

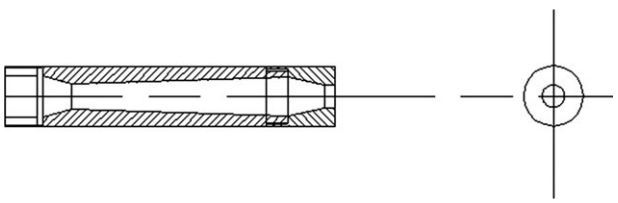

Figure 4. Diagram of the nozzle used in this study.

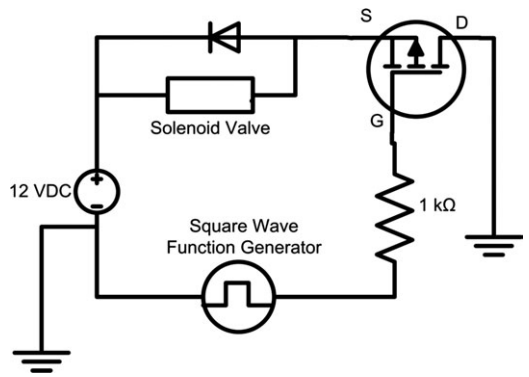

Figure 5. Circuit diagram of solenoid valve-based pulsation technique.

Sampling port

Samples of the bed material were taken from the bed after the atomized liquid injection using a sampling port 1.5 m above the distributor grid, on the opposite side of the bed from the nozzle (Figure 1). Each sample had an approximate mass of 500 g. These samples were then tested in two pieces of equipment: an avalanche machine and a moisture balance. The avalanche testing equipment consists of a rotating drum with a rotational speed of 0.3 rpm, which uses image recognition software to calculate how often the sample slips "avalanches" during the rotation. When the force of gravity overcomes the cohesive forces between the particles, the avalanche occurs; as such, the mean avalanche time (t_{av}) characterizes the powder cohesiveness.[17,18] In the moisture test, ~10 g of sample is introduced in the moisture balance, weighed, and then heated at 105°C until the weight is no longer changing.

Experimental Procedure

This section describes the methodology of the experiments that examined the effect of nozzle pulsations on the quality of a gas-atomized liquid injection. Several measurements were taken to determine the liquid-solid contact efficiency in the bed. Bed conductance measurements were collected, using the conductance probe. This conductance has been found to be proportional to the quality of liquid-solid mixing.[13]

The silica sand used in this study is a low-conductance particulate material and does not conduct electricity at a significant level when it is dry. However, when water is added, the wetted sand becomes relatively conductive. Wetted regions can become high conductance paths, which allows for the transmission of electrical current. When the water is distributed well throughout the system, there are more conductive paths for the electricity to flow, which results in an increased bed conductance. [13]

Before the start of each experiment, the superficial gas velocity of the fluidization air was set to 0.15 m/s. The solenoid valve circuit was completed, creating artificial fluctuations in the injection gas flow rate.

At the start of the experiment ($t = 0$ s), the water-mixed gas mixture was injected into the bed. The injection lasted for 10 s. The liquid and gas flow rates were set to the desired levels by adjusting the upstream pressure in the gas cylinders. The liquid flow rate was set so that the averaged flow rate was 2.2 kg/s, and so that 22 kg of water was injected in total. Because there was 8800 kg of silica sand in the bed, the maximum liquid-to-solid (L/S) ratio in the bed was 0.25 wt %, which does not significantly degrade the bed fluidization quality. An average (G/L) ratio of 0.8% was achieved, resulting in a gas flow rate of 0.176 kg/s.

At $t = 15$ s, the fluidization gas velocity was reduced to 0.075 m/s. The liquid was then allowed to mix for an additional 45 s. At $t = 1$ min, the fluidization gas was stopped, thus immediately defluidizing the bed. During this time, conductance measurements were taken, measuring how well the liquid was spread throughout the bed.

At $t = 10$ min, the bed was refluidized, at a superficial fluidization gas velocity of 0.12 m/s. It was then allowed to dry for 2 h, such that the bed would be completely dry and ready for the next experiment. Online measurements of bed temperature and conductance were used to ensure the bed was completely dry before each experiment, and that each experiment started at a constant temperature of 20°C.

Agglomerate sampling

Three 500 g samples of the sand within the bed were taken from a sampling port above the fluidized bed, at times $t = 11$, 15, and 20 min. These samples were then tested for free moisture content (the amount of liquid present in the sand that is not trapped in agglomerates) and for the presence of agglomerates in the sample. Most of results presented in this article were obtained with the samples taken at $t = 20$ min, because the 10 min of refluidization were necessary to achieve good mixing of the bed contents, so that the samples were representative of the whole bed.

In the evaporation test, a small amount (10 g or so) of each sample is weighed and then heated at 105°C, until the weight stops changing. The percentage change in mass is then recorded, as this is approximately the amount of total moisture (the sum of the amount of free moisture, microagglomerates, and macroagglomerates) present in the sample. This test is repeated three times for each sample.

In the avalanche test, about 300 g of a sample is placed in a rotating drum, and rotated at 0.3 rpm. Image recognition software detects when the sample slides ("avalanches") during the rotation. The test continues until the sample rotates 128 times, and the average avalanche time and the standard deviation of the avalanche time are recorded. This data can then be used to determine the microagglomerate, macroagglomerate, and free moisture content of the fluidized bed, as demonstrated in the next section.

Microagglomerate and macroagglomerate calculations

During the fluidized bed injection, much of the liquid gets trapped in liquid–solid agglomerates. In a reactor, these agglomerates restrict mass and heat transfer, and negatively affect the reactions in fluid cokers.[6] These agglomerates can be further divided into two subcategories: agglomerates that are small enough to fluidize together with the rest of the bed material (called microagglomerates), and agglomerates that are large and heavy and sink to the bottom of the fluidized bed (called macroagglomerates). Any injected liquid that does not agglomerate is known as free moisture. The free moisture and moisture in the agglomerates could then be expressed using a (L/S) ratio, which is a ratio between the mass of liquid present in the bed in the form described (free moisture, microagglomerate), and the total mass of solids of the bed. As such, the sum of the three (L/S) ratios should equal the overall liquid-solid ratio in the bed.

Preliminary experiments showed that the time between avalanches, which measures the powder cohesivity, is directly related to the free moisture, which makes the surface of the wet particles sticky, and is not affected by the presence of agglomerates. A correlation between the average time between avalanches and the free moisture content in the sample was derived from calibration data with mechanically mixed samples of known free moisture contents. This correlation is as follows:

$$\ln(L/S)_{\text{free moisture}} = 3.046 - 0.004626(t_{av})^{2.5} + 0.00148763(t_{av})^{3} \quad (2)$$

From this correlation, the free moisture content of the sample can be determined. Because macroagglomerates are by definition not fluidized, there are no macroagglomerates present in the sample. As such, the amount of microagglomerates present in the sample can be determined by subtracting

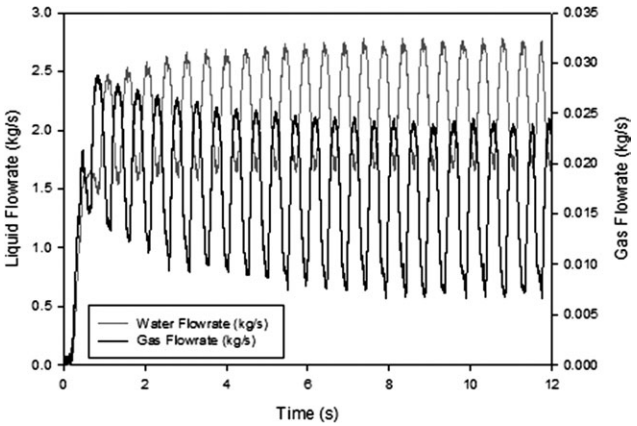

Figure 6. Liquid and gas flow rates during injection with 2-Hz pulsations with the BFC premixer and a volume of 12.5 mL between solenoid valve and restriction orifice.

the free moisture content from the total moisture content of the sample.

$$(L/S)_{\text{micro}} = (L/S)_{\text{total moisture, sample}} - (L/S)_{\text{free moisture}} \quad (3)$$

The bed is vigorously mixed when samples are taken, and it can be assumed that samples are representative of the material that is fluidized in the bed. The mass of solids trapped in the microagglomerates is considered insignificant, and the total solid content is assumed to be constant. As such, one can determine the macroagglomerate content in the bed from:

$$(L/S)_{\text{macro}} = (L/S)_{\text{total moisture, mass balance}} - (L/S)_{\text{total moisture, sample}} \quad (4)$$

This equation assumes that a negligible amount of solids is trapped in macroagglomerates, when compared to the total mass of solids in the bed. This assumption can be justified in view of the very large mass of solids in the bed and the relatively small mass of macroagglomerates. Therefore, the total moisture content of the bed can be calculated with a simple mass balance. The mass of liquid originally injected into the initially dry bed is known. The evaporation rate of liquid from the bed can be estimated by considering the following points:

- Fluidization air enters the system at a constant relative humidity of 12% as experimentally measured.
- Air is assumed to leave the fluidized bed saturated with water. Except for a short time during the initial injection, this is an accurate assumption as verified by humidity measurements of the air leaving the column.
- It is assumed that there is no drying during defluidization, when no air is flowing through the system.

First, the saturation pressure and saturation humidity were determined using Antoine's equation.

$$P_{\text{sat}} = e^{\left(23.44 - \frac{3965}{T+282.8}\right)} \quad (5)$$

$$h_{\text{sat}} = 0.6219\left(\frac{\frac{P_{\text{sat}}}{101325P_{\text{a}}}}{1 - \frac{P_{\text{sat}}}{101325P_{\text{a}}}}\right) \quad (6)$$

As the data acquisition also monitors the fluidization gas flow rate, one can use the difference between the saturation humidity and the inlet humidity to determine the rate of evaporation:

$$\text{Evaporation rate} = F_{\text{g}}(h_{\text{sat}} - h_{\text{in}}) \quad (7)$$

$$\left(\frac{L}{S}\right)_{\text{total moisture,mass balance}}(t) = \frac{m_{\text{liq, injected}} - \int_0^{\tau}(\text{Evaporation rate})dt}{m_{\text{solids}}} \quad (8)$$

Results

Figure 6 shows the effect of the pulsations on the liquid and gas flow rates during the injection, calculated from pressure data. The pressure measurements had been calibrated in extensive open-air testing. The pulsations are not shaped perfectly like the square waveform that is applied to the solenoid valve. This irregularity is caused by two factors. There is a volume between the solenoid valve and the restriction orifice and, when the solenoid valve is closed, the gas in this volume is gradually released through the orifice, causing the flow rate to decrease over time. This creates a capacitance effect, and it explains the reason for the residual gas flow when the solenoid valve is closed.

As expected, although the pulsations are applied only to the gas line, they greatly affect the liquid flow rate, as shown by Figure 6. A lower gas flow rate results in a smaller pressure drop through the spray nozzle, and, consequently, a lower pressure upstream of the premixer. As the pressure of the liquid tank is held constant, this reduction in downstream pressure increases the liquid flow rate.

The results shown in Figure 6 were obtained with the smallest volume between the solenoid valve and the restriction orifice (known as the "dead volume" or "capacitance"), which resulted in large pulsations. The gradual, slow decrease in the average gas flow rate, and conversely the increase in the liquid flow rate, is due to irregularities with the start-up of the injection. The injection length was 10 s so that the irregularities of the initial start-up could be considered insignificant relative to the steady-state flow rate.

Increasing the dead volume in the injection line led to a significant decrease in the amplitude of the pulsations. This can be seen in Figure 7, which illustrates the flow rates

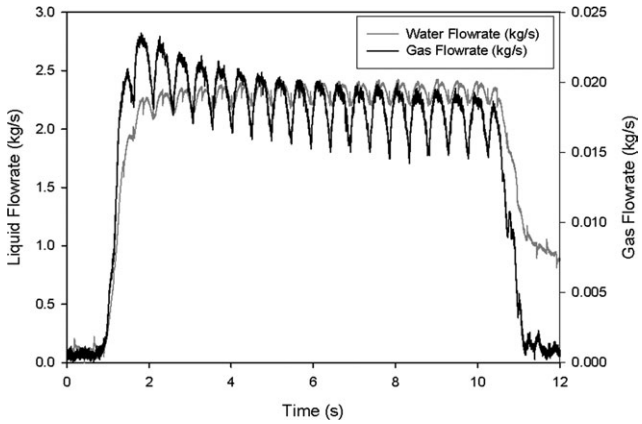

Figure 7. Liquid and gas flow rates during injection with 2-Hz pulsations in Type I nozzle with BFC premixer and a volume of 500 mL between solenoid valve and restriction orifice.

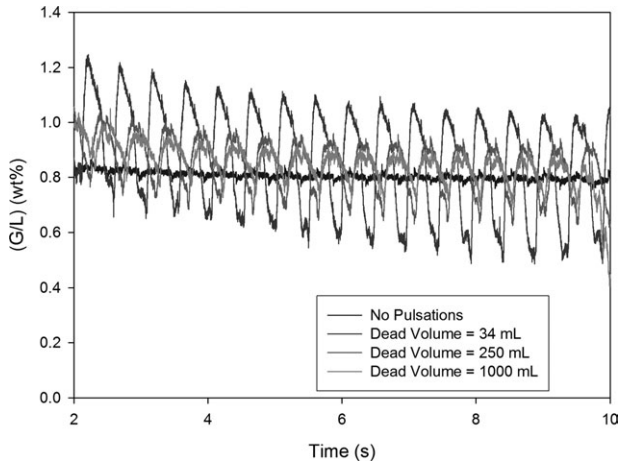

Figure 8. (G/L) ratios at various spacing volumes between the solenoid valve and the sonic nozzle.

2-Hz pulsations in Type I nozzle with BFC premixer, average (G/L) of 0.8 wt %.

found in a test where the spacing volume is increased from 34 to 500 mL. With this change, the pulsation amplitude decreases to approximately a third of the value seen with the smallest dead volume, as shown in Figure 6. The time-averaged flow rates of liquid and gas are held constant, so that a good comparison can be made between different tests.

The effect of changing the dead volume on the amplitude of the nozzle pulsations is shown in Figure 8. Varying dead volumes show different levels of variance in the (G/L) ratios. In Figure 9, the effect of changing the dead volume was plotted against the average amplitude of the pulsations for each experiment. The amplitude of pulsation was calculated as the distance between the extremes in the flow rate and the time-averaged flow rate. It was found that a strong logarithmic correlation was found between the two variables, with an R^2 value of 0.9862. Eventually, if the dead volume is sufficiently large, the amplitude of the pulsations will be insignificant enough that the system will resemble the case in which no pulsations are used.

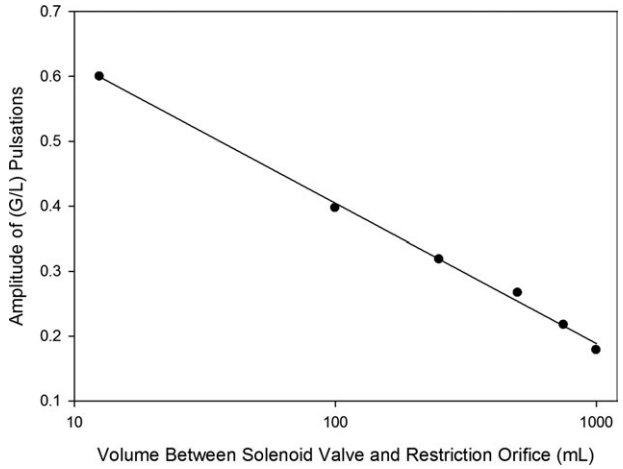

Figure 9. The effect of changing the volume between the solenoid valve and restriction orifice on the amplitude of the nozzle pulsations.

2-Hz pulsations in Type I nozzle with BFC premixer, average (G/L) of 0.8 wt %.The amplitude was obtained from Figure 8 and is expressed in wt%.

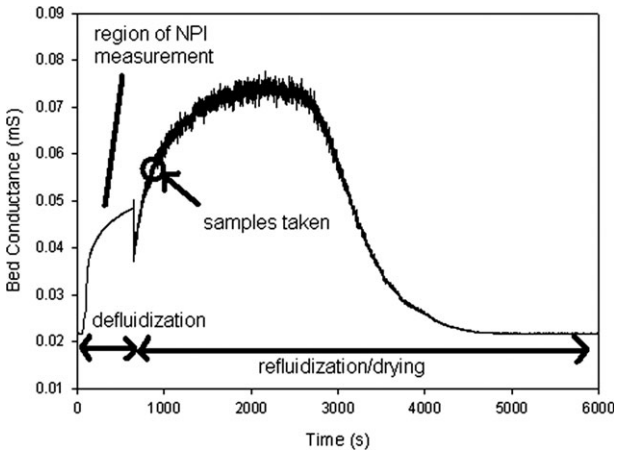

Figure 10. Conductance probe signal, including defluidization and refluidization (drying) zones.

The conductance of the fluidized bed solids over the course of an experimental run, as measured by the conductance probe is displayed in Figure 10. For the first 10 min of the experiment, the bed is defluidized, and the bed conductance, as measured by the probe, increases logarithmically. The nozzle performance index (NPI), used in a previous work by the authors,[14] is defined as the slope of this logarithmic curve: a high NPI value means that water diffuses quickly through the defluidized bed, increasing the bed conductance quickly. A high NPI therefore corresponds to a good original distribution of the liquid on the bed particles, just before defluidization. After this point, the bed is refluidized, allowing the agglomerates to break, and the bed solids to dry: just after refluidization, the conductance increases as the rate at which moisture is dispersed from broken agglomerates is greater than the evaporation rate; the conductance then peaks and decreases as the drying rate becomes predominant. As seen in the graph, the defluidization technique is used because there is much less noise in the probe signal than when the bed is fluidized. Samples are taken 10 min after the bed is refluidized, because the liquid and agglomerates have not moved through the unit sufficiently at the time of refluidization for accurate sampling.

Effect of pulsation amplitude

The effects of the variation in the amplitude of the pulsations on the quality of the injection and the spreading of liquid, as characterized by the NPI, are displayed in Figure 11. The amplitude is plotted against both the NPI and the free moisture content (which is calculated using Eq. 2). Both sets of data show that the nozzle performance is maximized for the largest of the tested pulsation amplitudes. The data where no pulsations are applied are displayed on the far left of the plot. This corresponds to a pulsation amplitude of about 0.1 wt % (G/L), as there are still small natural fluctuations in the gas flow rate, even when artificial pulsations are not applied. When the amplitude of the pulsations becomes small, the nozzle performance decreases to the same level as a test with no pulsations.

One possible explanation for the beneficial impact of the pulsations is that changing (G/L) ratio also changes the jet penetration depth of the injection.[19] As most of the liquid from the injection is deposited at the end of the jet cavity[2] changing the jet penetration depth leads to a greater spread

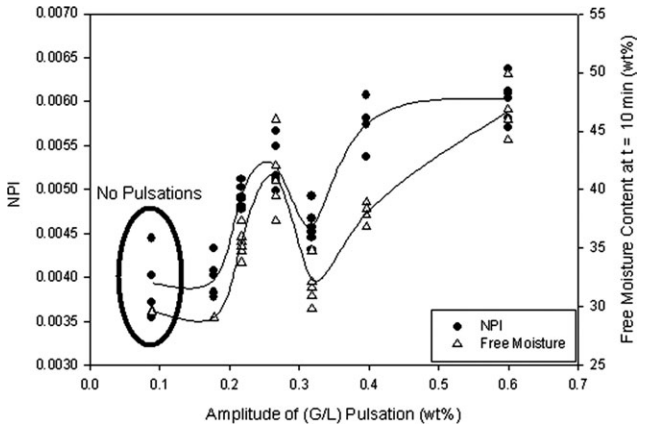

Figure 11. Effect of changing the amplitude of the nozzle pulsation on the nozzle performance.

2-Hz pulsations in Type I nozzle with BFC premixer, average (G/L) of 0.8 wt %.

of liquid throughout the fluidized bed, resulting less agglomerate formation and a higher free moisture content. The pulsations also affect the liquid droplet size: as a result of the pulsations, more liquid is injected in the form of larger droplets: as demonstrated in a previous work by the authors,[13] small (G/L) ratios result in larger droplets, which is not beneficial to the liquid distribution. There are, therefore, two opposing results of the pulsations: the beneficial variation in jet penetration, and the larger droplet size. This may explain the complex and unexpected behavior shown in Figure 11. As such, there is a balance to be found when choosing the optimal pulsation amplitude.

Very similar trends in the effects of the amplitude of the pulsations on NPI and free moisture content have been observed and illustrated in Figure 11. To further compare these two variables, a plot was constructed comparing these two characteristic parameters (Figure 12). This plot used the data points from all the experiments used in this work, including the tests varying the amplitude, frequency, and (G/L), as well different nozzle configurations. A fairly strong linear correlation was found between the two variables ($R^2 = 0.8032$). This shows some evidence that the NPI is an indication of how well moisture is spread throughout the unit, as was hypothesized in previous studies by the authors.[14,16]

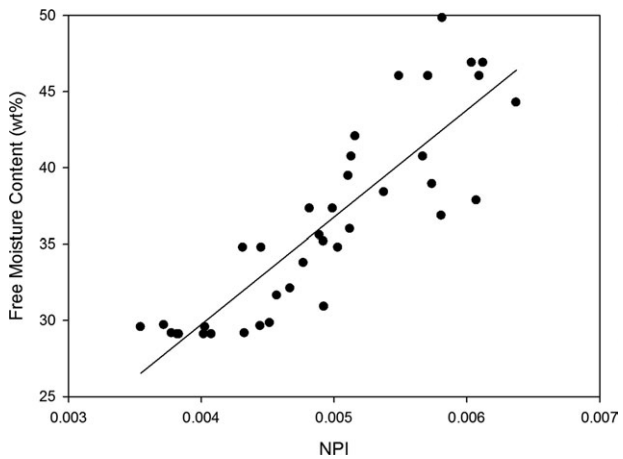

Figure 12. Correlation between free moisture content in fluidized bed and NPI. $R^2 = 0.8032$.

This seems to confirm that the NPI is a very useful tool for determining the quality of an injection, because the free moisture content of the bed leads to increased liquid-solid contact within the bed, which is critical for important industrial processes, such as fluid coking and FCC. The strong correlation between NPI and free moisture content was also noted in a previous work using the active conductance technique.[13,14]

The concentration of microagglomerates (the agglomerates that remain fluidized, as defined in Eq. 3) found in the fluidized bed at different pulsation amplitudes is presented in Figure 13. Once again, the points on the far left represent the base case, for which no pulsations were applied. Microagglomerates are small agglomerates that can still be fluidized, and cause a much less significant mass transfer limitation than the larger macroagglomerates. The microagglomerate content decreases greatly in the midrange amplitudes of about 0.2–0.3 wt % (G/L). This corresponds to the sudden increase in free moisture and NPI found in Figure 11. With the exception of these midrange amplitudes, the microagglomerate content displays a steady decrease with increasing nozzle fluctuations, displaying the benefits of larger pulsations.

In Figure 13, the microagglomerate content (agglomerates that remain fluidized, as calculated in Eq. 4) at amplitudes of 0.6 wt % (G/L) and 0.3 wt % (G/L) are approximately identical. However, the nozzle performance and free moisture contents are much higher in the case of the larger pulsations. This is due to the higher macroagglomerate content at the lower pulsation amplitude, as seen in Figure 14. At the same point where the microagglomerate content suddenly decreases, the macroagglomerate content increases. At this point, while the free moisture content (and as such, liquid-solid contact efficiency) are increasing, these extra macroagglomerates are also limiting the mass transfer in the bed, as well as potentially causing unwanted defluidized areas of the bed. This increase in macroagglomerates could be what was detected in previous studies that led to identifying the negative consequences of the pulsations.[10,11] However, when the amplitude of the pulsations increases, the macroagglomerate and microagglomerate contents decrease, leading to higher free moisture content. Consequently, the largest pulsations

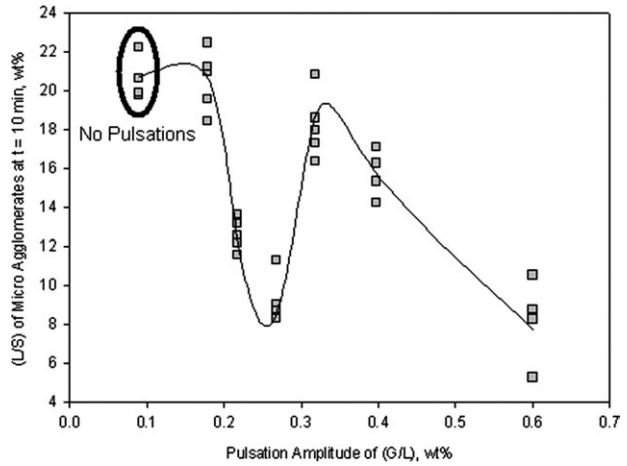

Figure 13. Microagglomerate (Eq. 3) content of bed after 10 min of refluidization.

2-Hz pulsations in Type I nozzle with BFC premixer, average (G/L) of 0.8 wt %.

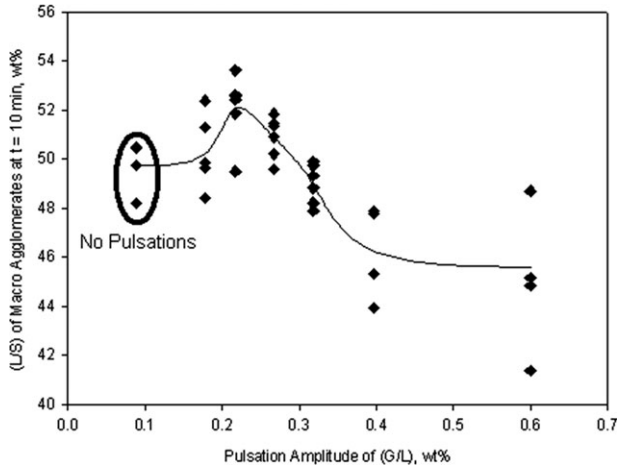

Figure 14. Macroagglomerate (Eq. 4) content of bed after 10 min of refluidization.

2-Hz pulsations in Type I nozzle with BFC premixer, average (G/L) of 0.8 wt %.

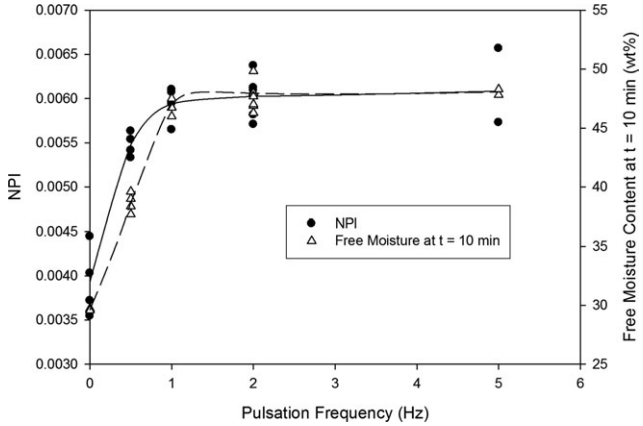

Figure 16. The effect of pulsation frequency on nozzle performance.

Average (G/L) ratio of 0.8 wt %, pulsation amplitude of 0.6 wt % (G/L).

are the most beneficial, as compared to the midrange pulsations that show high free moisture content but also high macroagglomerate counts.

In Figure 15, the results presented in the previous figures, which represent data from the pilot-scale unit, are compared to results from a smaller scale unit. Similar nozzle and premixer geometries are used in both cases, with a scaling factor of 16 (the internal diameters of the nozzles are 16 times larger on the large scale than the small scale). The same (G/L) ratio is used, even though the individual gas and liquid flow rates, as well as the bed mass, are much smaller. As one can see, a similar trend is apparent in both cases, although the small scale tests exhibit a higher NPI. However, both sets of experiments show that the nozzle performance increases as the gas pulsations become more pronounced.

Effect of pulsation frequency

The effect of changing the pulsation frequency on the nozzle performance is illustrated in Figure 16. A frequency of 0 Hz represents the case where no pulsations are applied to the gas line. The graph shows that a great improvement in nozzle performance occurs when pulsations are applied to the apparatus, but the quality of the jet–bed interaction seems mostly unaffected by the change in the pulsation frequency. Performance at a frequency of 0.5 Hz is slightly poorer than at higher frequencies. This is consistent with attribution of the beneficial effect of pulsations to variations in jet penetration. At 0.5 Hz, the jet remains stationary for a longer period of time and too much liquid is therefore deposited in one limited area. At frequencies ranging from 1 to 5 Hz, the NPI and free moisture content show a tremendous increase, nearly doubling in magnitude when pulsations are applied.

Figure 17 summarizes the effect of different pulsation frequencies on liquid–solid agglomeration, for a pulsation amplitude of 0.6 wt %. The increase in free moisture caused by inducing pulsations seems to have a close, inverse relationship with the decrease in unwanted macroagglomerates under

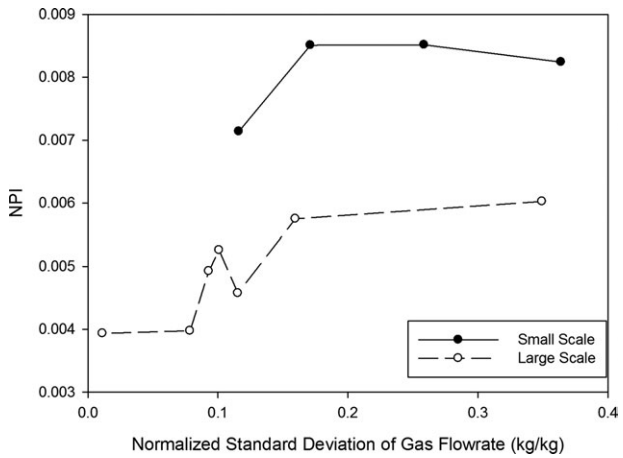

Figure 15. Comparison amplitude tests in small and large scale units.

Type I nozzle and BFC premixer used in both cases, with an average (G/L) ratio of 0.8%. Scaling factor of 16 between large and small scale nozzles.

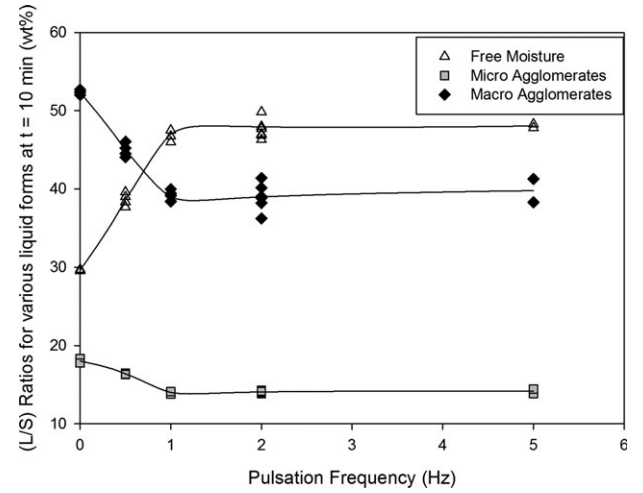

Figure 17. Agglomeration occurring after 10 min refluidization, with various pulsation frequencies.

Average (G/L) ratio of 0.8 wt %, pulsation amplitude of 0.6 wt % (G/L).

the same conditions. There is also a decrease in microagglomerates at the same point.

The effect of frequency is similar in both the small scale and large scale units, as seen in Figure 18. In both units, the pulsation frequency does not seem to matter, as long as it is higher than 1 Hz.

Effect of different premixers

To test the versatility of the pulsation technique, a different type of premixer, the W premixer, was used. These results can be seen in Figure 19. It shows a similar increase in nozzle performance when pulsations are applied as in the case of the BFC premixer. Under the current operating conditions, the BFC shows a slightly improved nozzle performance over the W premixer, both with and without pulsations. The difference between the NPI when pulsations are applied shows that the conductance probe signal does not saturate, even at these high conductance levels. Once again, the W premixer is insensitive to frequency changes at the high frequencies, showing that the transient periods in between pulsations are unimportant.

There are limitations that prevent the current technique from being used in an industrial setting. However, there are several options on how to implement artificial pulsations in an industrially viable fashion. Technology similar to that used in modern diesel fuel injectors could be used. These techniques include the use of piezo-actuated control valves, in which an applied electrical field causes a material to expand, opening a valve.[20] It has also been found[21] that similar sprays patterns, if not better spray patterns, can be formed from a piezo-actuated valve as compared to a solenoid-induced control valve. A similar waveform could be applied to the one used in this study, to induce pulsations. This technique would be less prone to breaking than a solenoid valve setup, as there are less delicate parts, such as the spring and solenoid coil.

Conclusions

Pulsations can be used to dramatically improve the distribution of liquid sprayed in a large-scale fluidized bed unit.

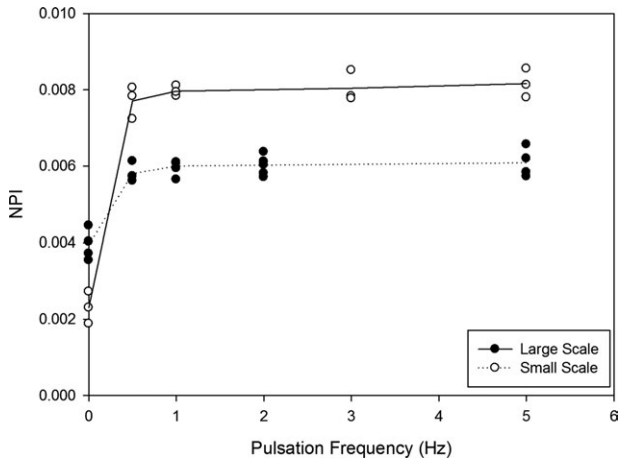

Figure 18. A comparison of the effect of pulsation frequency on small and large-scale fluidized beds.

Type I nozzle and BFC premixer, average (G/L) of 0.8 wt % used.

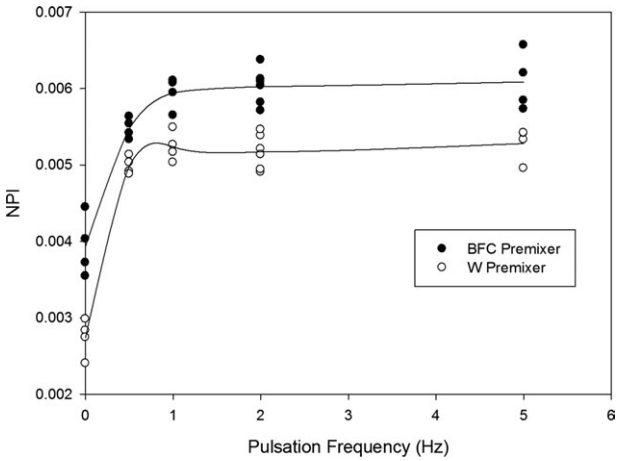

Figure 19. Comparison of BFC and W premixers.

Type I nozzle, 12.5-mL dead volume, 0.8% average (G/L), 2-Hz pulsation frequency.

The small-scale pulsations experiments were successfully scaled up to a larger scale, showing the industrial viability of applying pulsations, as well as the versatility of this method.

Pulsations frequencies ranging from 1 to 5 Hz are highly beneficial and there is little effect of frequency in this range. Large pulsation amplitudes led to less agglomerate formation and better liquid-solid contact throughout the fluidized bed.

Two types of premixers were tested, and it was found that the effects of pulsations on nozzle performance were similar with both configurations. This helped to demonstrate the versatility of the pulsation technique as a method to improve gas–liquid injections.

Last, using analysis of bed samples, it was found that there was a strong correlation between the NPI used in previous studies and the free moisture content found in the bed, shortly after refluidization. As free moisture is the most beneficial form of liquid within the fluidized bed, this correlation shows that the NPI is a useful tool in determining the quality of liquid spreading throughout the bed solids.

Literature Cited

1. Song X, Bi H, Jim Lim C, Grace J, Chan E, Knapper B, McKnight C. Hydrodynamics of the reactor section in fluid cokers. *Powder Technol*. 2004;147:126–136.
2. House P, Saberian M, Briens C, Berruti F, Chan E. Injection of a liquid spray into a fluidized bed: particle-liquid mixing and impact on fluid coker yields. *Ind Eng Chem Res*. 2004;43:5663–5669.
3. Leclère K, Briens C, Gauthier T, Bayle J, Guigon P, Bergougnou M. *Experimental Study of the Vaporization of Liquid Droplets Injected into a Gas-Solid Fluidized Bed, GLS'6*. Vancouver: Canadian Society for Chemical Engineering, 2003.
4. Bruhns S, Werther J. An investigation of the mechanism of liquid injection into fluidized beds. *AIChE J*. 2005;51:766–775.
5. Knapper B, Gray M, Chan E, Mikula, R. Measurement of efficiency of distribution of liquid feed in a gas-solid fluidized bed reactor. *Int J Chem React Eng*. 2003;1:1–11.
6. Weber S, Briens C, Berruti F, Chan E, Gray M. Agglomerate stability in fluidized beds of glass beads and silica sand. *Powder Technol*. 2006;165:115–127.
7. Ariyapadi S, Holdsworth D, Norley C, Berruti F, Briens C. Digital X-ray imaging technique to study the horizontal injection of gas-liquid jets into fluidized beds. *Int J Chem React Eng*. 2003;1:1–16.
8. Hulet C, Briens C, Berruti F, Chan EW, Ariyapadi S. Entrainment and stability of a horizontal gas-liquid jet in a fluidized bed. *Int J Chem React Eng*. 2003;1:1–13.

9. Ariyapadi S, Berruti F, Briens C, Griffith P, Hulet C. Modeling the injection of gas-liquid jets into fluidized beds of fine particles. *Can J Chem Eng*. 2003;81:891–899.
10. Ariyapadi S, Berruti F, Briens C, Knapper B, Skwarok R, Chan E. Stability of horizontal gas-liquid sprays in open air and in a gas-solid fluidized bed. *Powder Technol*. 2005;155:161–174.
11. McDougall S, Saberian M, Briens C, Berruti F, Chan E. Effect of liquid properties on the agglomerating tendency of a wet gas-solid fluidized bed. *Powder Technol*. 2005;149:61–67.
12. Sabouni R, Leach A, Briens C, Berruti F. Enhancement of the liquid feed distribution in gas-solid fluidized beds by nozzle fluctuations. *AIChE J*. 2011;57:3344–3350.
13. Portoghese F, House P, Berruti F, Briens C, Adamiak K, Chan E. Electric conductance method to study the contact of injected liquid with fluidized particles. *AIChE J*. 2008;54:1770–1781.
14. Leach A, Chaplin G, Briens C, Berruti F. Comparison of the performance of liquid–gas injection nozzles in a gas–solid fluidized bed. *Chem Eng Process*. 2009;48:780–788.
15. Base TE, Chan EW, Kennett RD, Emberley DA. US Patent No. 6,003,789, 1999. Washington, DC: US Patent and Trademark Office.
16. Leach A, Portoghese F, Briens C, Berruti F. A new and rapid method for the evaluation of the liquid-solid contact resulting from liquid injection into a fluidized bed. *Powder Technol*. 2007;184:44–51.
17. Lavoie F, Cartillier L, Thibert R. New methods characterizing avalanche behavior to determine powder flow. *Pharma Res*. 2002;19:887–893.
18. Lee Y, Poynter R, Podczeck F, Newton J. Development of dual approach to assess powder flow from avalanching behavior. *AAPS PharmSciTech* 2000;1:44–52.
19. Ariyapadi S, Berruti F, Briens C, McMillan J, Zhou D. Horizontal penetration of gas-liquid spray jets in gas-solid fluidized beds, *Int J Chem React Eng*. 2004;2:1–13.
20. Suh HK, Park SW, Lee CS. Effect of piezo-driven injection system on the macroscopic and microscopic atomization characteristics of diesel fuel spray. *Fuel* 2007;86:2833–2845.
21. Chung NH, Oh BG, Sunwoo MH. Modelling and injection rate estimation of common-rail injectors for direct-injection diesel engines. *J Automobile Eng*. 2008;222D:1089–1101.

Manuscript received Jan. 24, 2012, revision received Apr. 11, 2012, and final revision received Jun. 9, 2012.